Percolative superconductivity in highly underdoped $La_{2-x}Sr_xCuO4$ thin films

I. Zajcewa[1], I. Abaloszewa[1], M. Chrobak[2,3], Š. Chromik[4], M. Talacko[4], M. Špankova[4], P. Gierłowski[1], M. Z. Cieplak[1]

[1] Institute of Physics, Polish Academy of Sciences, 02 668 Warsaw, Poland
[2] AGH University of Science and Technology, Faculty of Physics and Applied Computer Science, Solid State Physics Department, al. A. Mickiewicza 30, 30-059, Krakow, Poland.
[3] AGH University of Science and Technology, Academic Center for Materials and Nanotechnology, al. A. Mickiewicza 30, 30-059 Krakow, Poland.
[4] Institute of Electrical Engineering SAV, Dúbravská cesta 9, 84104 Bratislava, Slovakia

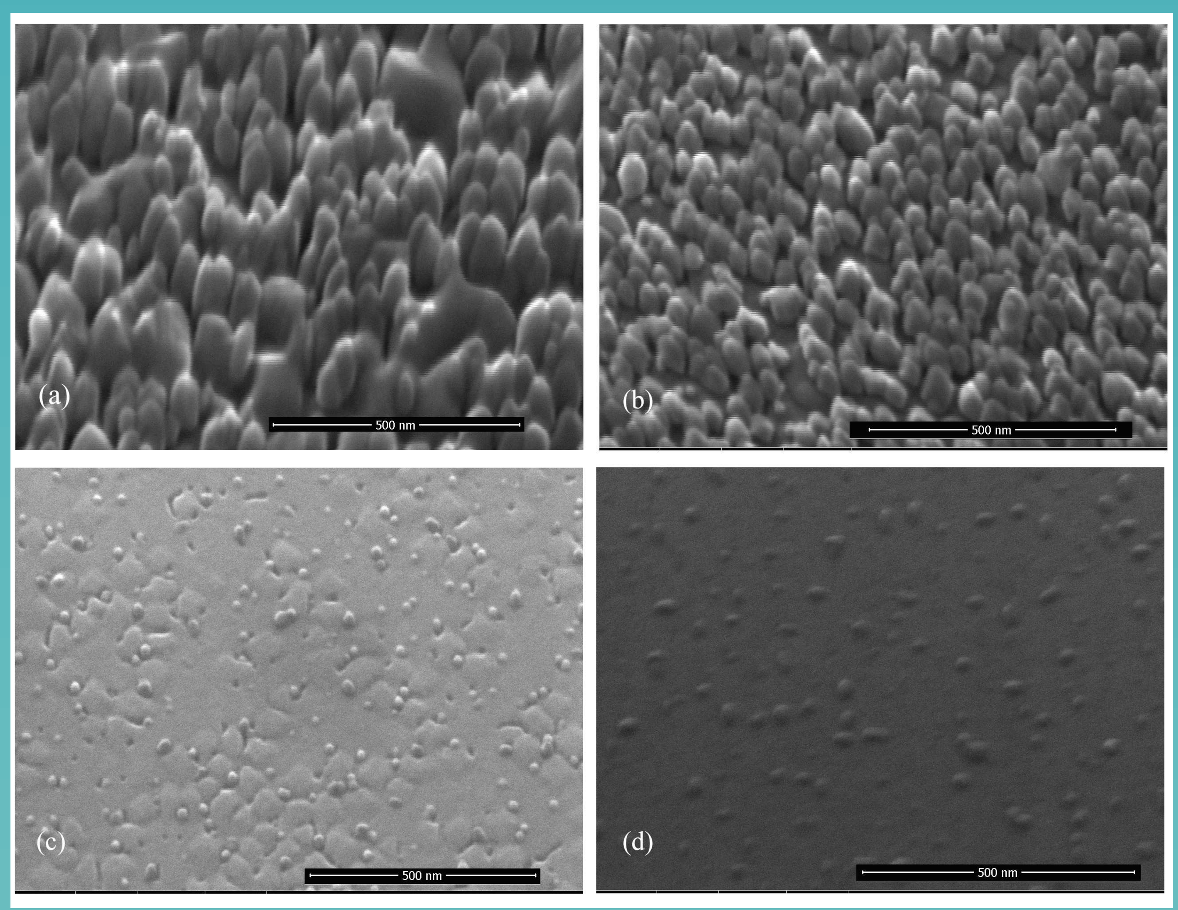

SEM images for films: with $x = 0.06$ (a) $T_c^{on} = 11.8$K; (b) $T_c^{on} = 15.2$K; $x = 0.048$ (c) $d \approx 60$nm, $T_c^{on} = 16.8$K; (d) $d \approx 20$nm, $T_c^{on} = 26.4$K;

Epitaxial $La_{2-x}Sr_xCuO_4$ (LSCO) thin films were deposited from stoichiometric ceramic target by pulsed laser deposition (PLD) using Nd:YAG laser (λ = 266 nm), with repetition rate 1Hz and energy density 1.3 J/cm² at the target surface. The targets with the Sr content $x = 0.045 \div 0.06$ were used, among which the ones with $x = 0.045 \div 0.051$ are not superconducting in the bulk. The films were grown on $SrLaAlO_4$ (SLAO) substrates. During deposition the substrates were held at temperature 760^{0}C in the oxygen atmosphere of 300mTorr. After deposition, the O_2 pressure in the chamber was increased to 500Torr, and the films were slowly cooled down to room temperature with a rate of 3K per minute.

First, on the pristine film the silver contacts were deposited by evaporation in vacuum. For transport measurements the films were patterned photolithographically into Hall bar structure with 2 mm long and 200 µm wide current path, and standard four-probe measuring method was used.

The images of the surfes of the films were obtained by using a scanning electron microscope (SEM) FEG250, with resolution of 1.2 nm equipped with SE and BSE detector with possibility to measure in environmental mode (for non-conductive samples).

Superconducting transition temperature and magnetoresistance were measured on photolithographically patterned films using a standard four-probe method at temperatures down to 50 mK and in fields up to 14 T (with current I = 100 nA), and current-voltage characteristics (IVC) measurements were performed in Closed Cycle Dilution Refrigerator TRITON (DR) from Oxford Instruments using low frequency lock-in technique. To minimize Joule heating, the IVC were measured using rectangular current pulses, with a current-on time of 50 ms and current-off time of 100 ms.

The effective medium theory (EMT) was used to describe temperature dependencies of resistance of films near the transition to superconducting state. Experimental dependencies of R(T) were fitted by equation:

$$R(T) = R^{\infty}\left[w \cdot erf\left(\frac{T - \overline{T_c}}{\sqrt{2}\gamma}\right) + 1 - w\right], \qquad (*)$$

where $erf(x) = \frac{2}{\sqrt{\pi}}\int_0^x e^{-z^2}dz$ - is the error function;

w - the weight of the T_c distribution represents the fraction of SC puddles, parameterized by its mean value, $\overline{T_c}$ and its width, γ; 1-w - non-SC fraction represents the metallic background [S. Caprara et. al., Supercond. Sci. Technol. 28, 014002 (2015)].

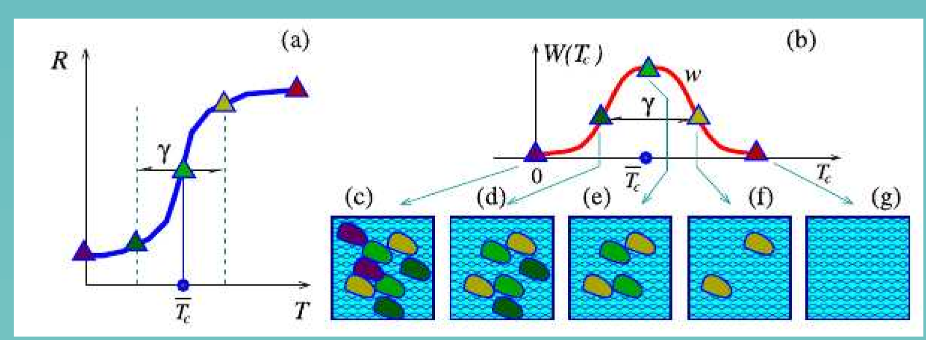

(a) Sketch of the behavior of the resistance as a function of temperature in a case when the superconducting fraction does not percolate.
(b) Distribution of critical temperatures W (T_c) in the superconducting puddles, which occupy a fraction, w, of the sample; the remaining 1 − w fraction will never become superconducting. (c-g) When the temperature is reduced from (g) to (c), superconducting puddles appear in the system as soon as the local critical temperature exceeds T. However, if the puddles do not percolate down to T = 0, the global zero resistance state is never reached.

[S. Caprara et. al., Supercond. Sci. Technol. 28, 014002 (2015)].

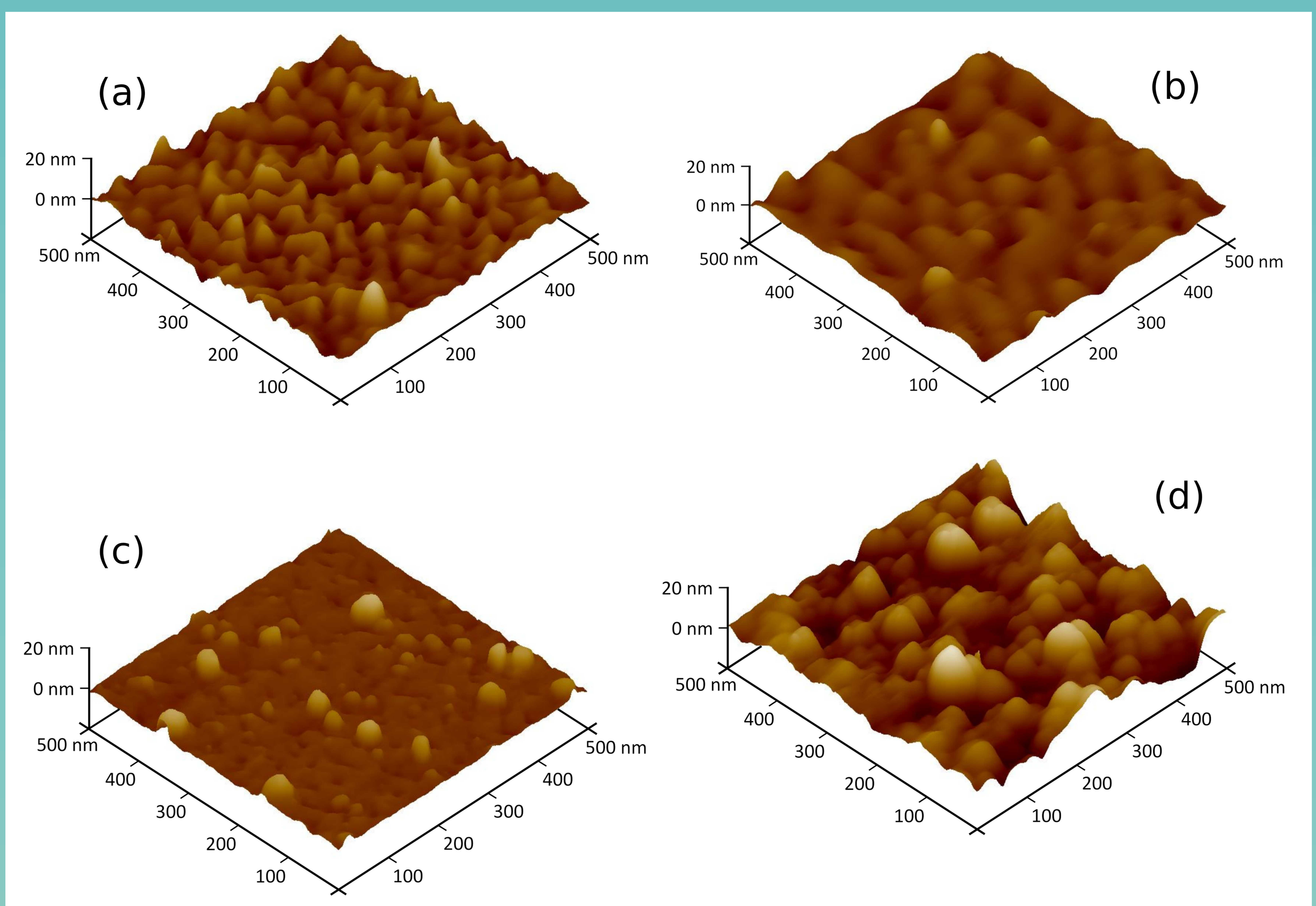

AFM images for films

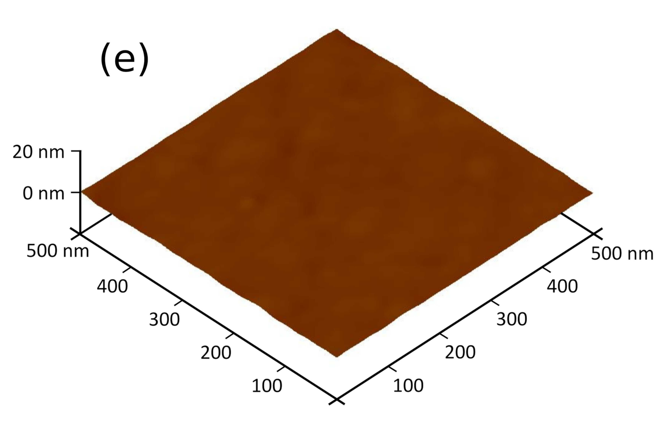

(a) double layer: $x = 0.135$, d = 100 nm on the bottom, and $x = 0.045$, d = 12 nm on the top, T_c^{on} = 13.3K;

(b) $x = 0.135$, d = 100 nm, T_c^{on} = 31K;

(c) $x = 0.045$, d = 12 nm, T_c^{on} = 14K; ε = 0.493

(d) $x = 0.045$, d = 100 nm, T_c^{on} = 0.

(e) $x = 0.045$, d = 12 nm, T_c^{on} = 24K; ε = 0.335

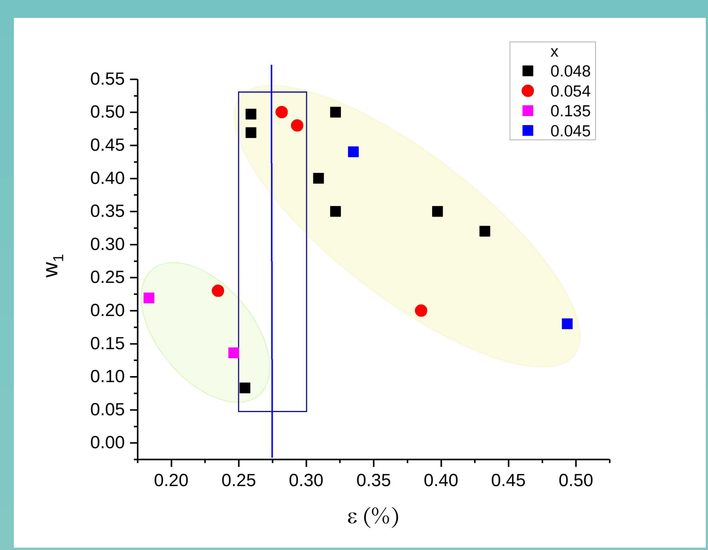

The weight of the T_{c1} distribution vs strain, ε

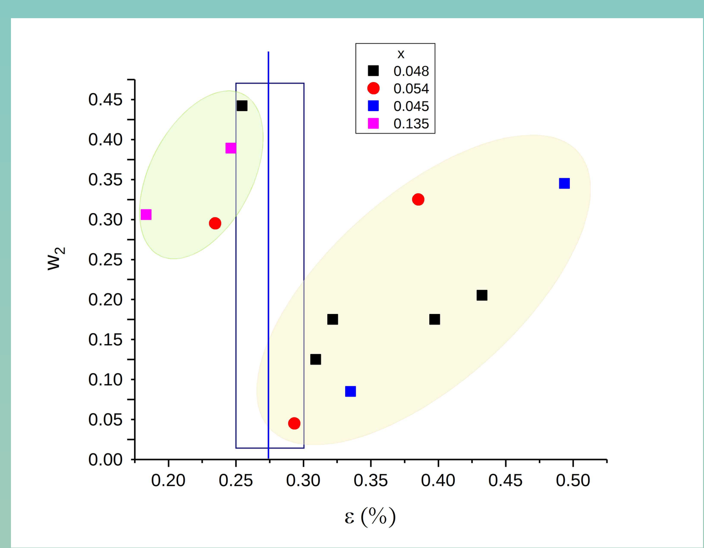

The weight of the T_{c2} distribution vs strain, ε

Temperature dependences for our samples was fitted with the EM theory assuming the existence of two types of SC puddles with T_{c1} and T_{c2}, $T_{c1} > T_{c2}$. The transition temperature, T_c, extracted from experiment lies between these two temperatures, $T_{c1} > T_c > T_{c2}$. The temperature dependences for some fraction of the films were fitted using only one w, what could be the consequence of greater homogeneity of the samples.

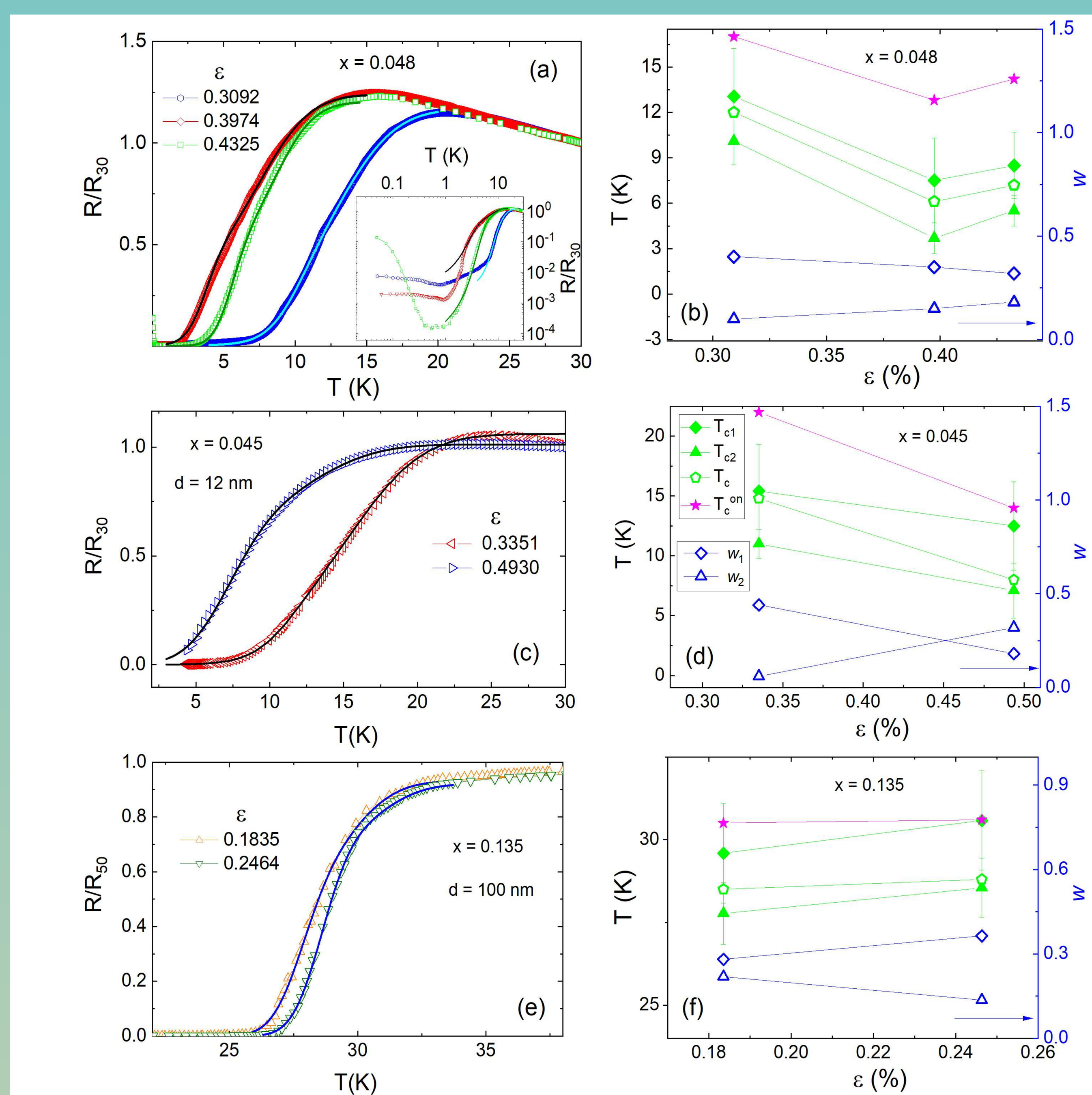

Normalized resistance R/R_{30} vs T: (a) for films with thicknesses 65 nm, 48 nm and 38 nm for $x = 0.048$; (c) for films with thicknesses 12 nm and 15 nm for $x = 0.045$; (e) for films with thickness 100 nm for $x = 0.135$. Lines in (a), (c) and (e) show results of fitting by equation (*); insert in (a) shows R/R_{30} vs T in log-log scale. On (b), (d) and (f): the dependences of fitting parameters vs strain (right blue side); the dependences of transition temperatures from the experiments and form the fitting vs strain (left black side).

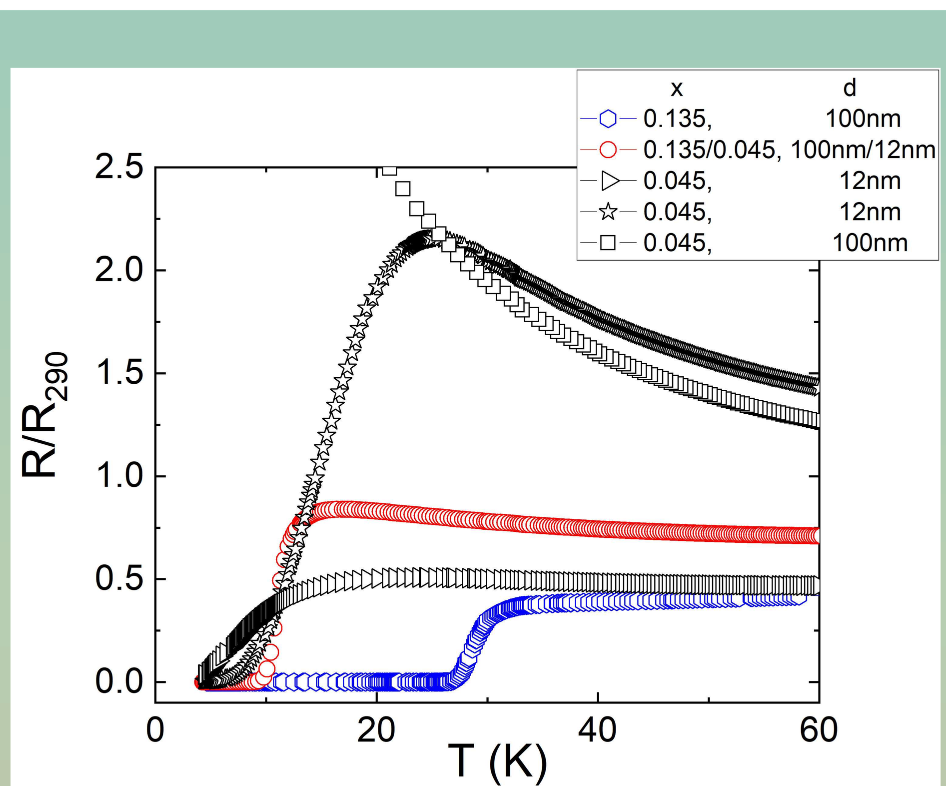

The temperature dependence of the resistance normalized to the resistance at T = 290K, R/R_{290}.

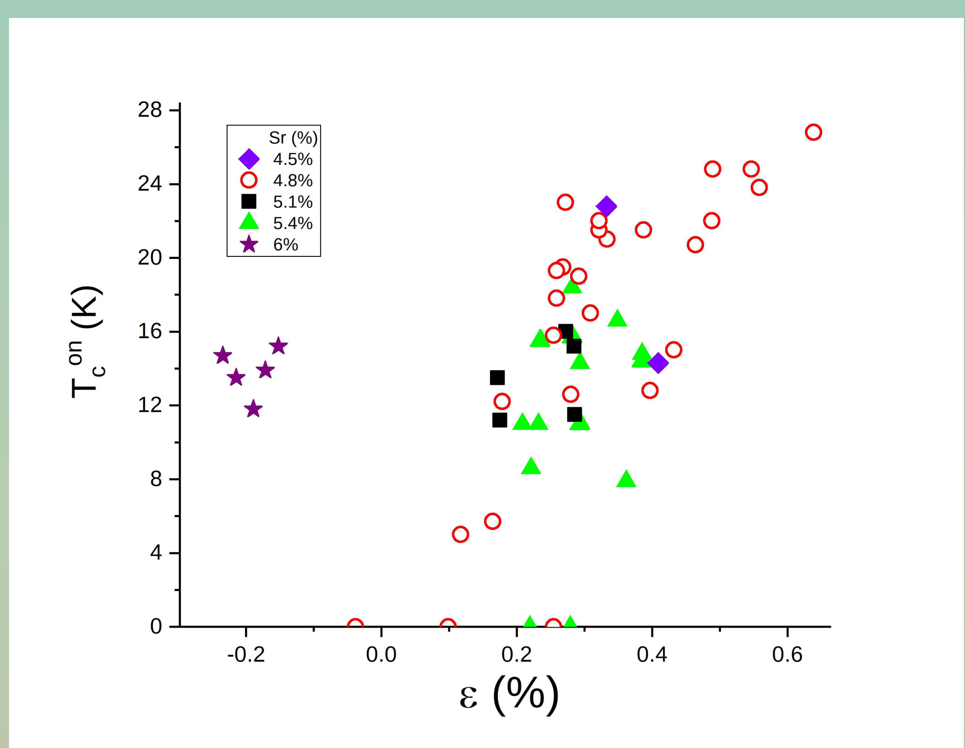

T_c^{on} as a function of strain, ε.

Targets with $x = 0.045$, 0.048 and 0.051 - are non superconducting.
T_c^{on} = 6.2K – for target with $x = 0.054$;
T_c^{on} = 20K - for target with $x = 0.06$.

Here ε is the strain induced by the lattice mismatch quantified using the definition, $\varepsilon_l = \frac{l_{film} - l_{bulk}}{l_{bulk}} 100\%$ where l is the lattice parameters value.

The transition temperature T_c^{on} - the temperature at which the resistance starts to deviate from the normal state resistance.

The most stressed films with highest T_c^{on} have the smoothest surface and the films wiht tensile strain have the surface in the form of columns.

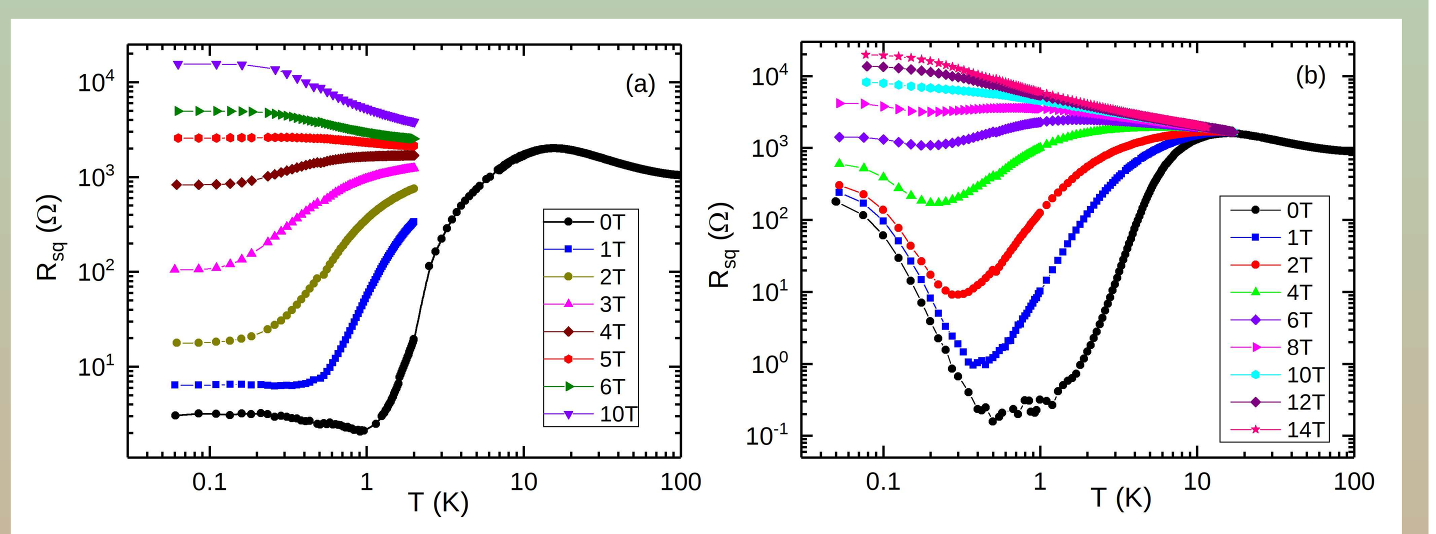

R_{sq} vs T on a log–log scale, for B in the range of 0 - 14 T, for three films with $x = 0.048$: (a) d = 48 nm, ε = 0.3974; (b) d = 38 nm, ε = 0.4325.

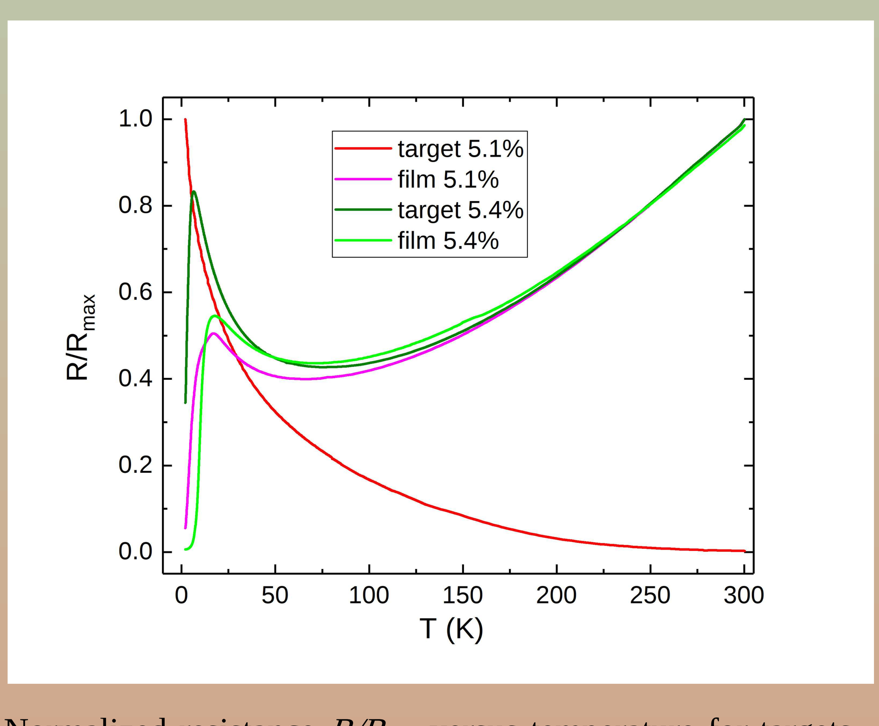

Normalized resistance R/R_{max} versus temperature for targets and films, deposited from this targets, with doping $x = 0.051$ and $x = 0.054$

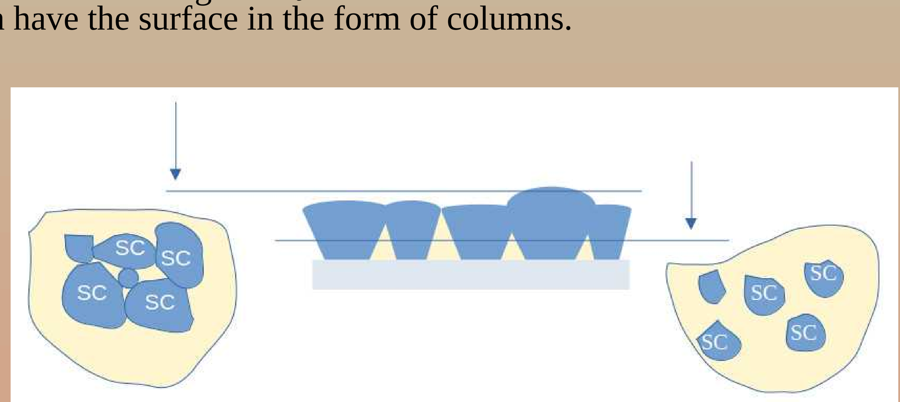

Simplified diagram of the grown film

Compressive strain in a plane of the strongly underdoped LSCO films with low carrier concentration causes the formation of the areas with uneven carrier distribution. As a result, a network of SC areas is formed, which are intermixed with metallic/insulating areas.

The evolution of resistance with temperature and magnetic field supports the scenario of inhomogeneous superconductivity, resembling a disordered array of superconducting islands immersed in a nonsuperconducting matrix.

The transition to superconducting state studied here is successfully described by the effective medium theory assuming that the sample is broken up into large macroscopic superconducting "puddles". However, this theory it is not suitable for the description of the resistance if dR/dT is negative ("insulating") below the T_c.

Acknowledgments: We would like to thank M. Berkowski and M. Głowacki for substrate preparation and M. Ożga for sharing AFM images of films. This work has been supported by Polish NSC Grant No.DEC-2018/02/X/ST3/00582.